BIOCHEMISTRY
including biophysical chemistry & molecular biology

ARTICLE

pubs.acs.org/biochemistry

Dissociation of Apolipoprotein E Oligomers to Monomer Is Required for High-Affinity Binding to Phospholipid Vesicles

Kanchan Garai, Berevan Baban, and Carl Frieden*

Department of Biochemistry and Molecular Biophysics, Washington University School of Medicine, St. Louis, Missouri 63110, United States

ABSTRACT: The apolipoprotein apoE plays a key role in cholesterol and lipid metabolism. There are three isoforms of this protein, one of which, apoE4, is the major risk factor for Alzheimer's disease. At micromolar concentrations all lipid-free apoE isoforms exist primarily as monomers, dimers, and tetramers. However, the molecular weight form of apoE that binds to lipid has not been clearly defined. We have examined the role of self-association of apoE with respect to interactions with phospholipids. Measurements of the time dependence of turbidity clearance of small unilamellar vesicles of dimyristoyl-*sn*-glycero-3-phosphocholine (DMPC) upon addition of apoE show that higher molecular weight oligomers bind poorly if at all. The kinetic data can be described by a reaction model in which tetramers and dimers of apoE must first dissociate to monomers which then bind to the liposome surface in a fast and reversible manner. A slow but not readily reversible conformational conversion of the monomer then occurs. Prior knowledge of the rate constants for the association−dissociation process allows us to determine the rate constant of the conformational conversion. This rate constant is isoform dependent and appears to correlate with the stability of the apoE isoforms with the rate of dissociation of the apoE oligomers to monomers being the rate-limiting process for lipidation. Differences in the lipidation kinetics between the apoE isoforms arise from their differences in the self-association behavior leading to the conclusion that self-association behavior may influence biological functions of apoE in an isoform-dependent manner.

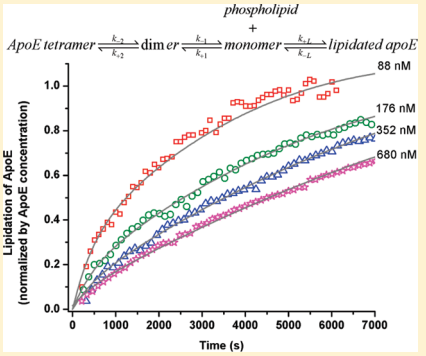

Apolipoprotein E (apoE) is a constituent of several plasma lipoproteins and plays a key role in the metabolism of cholesterol and triglycerides. There are three isoforms of the protein (apoE2, apoE3, and apoE4) that differ only by single amino acid changes. These isoforms differ markedly in their preferences for lipoprotein particles in the plasma and in their receptor binding abilities.[1−3] In brief, apoE2 and apoE3 bind preferentially to high-density lipoprotein (HDL) particles whereas apoE4 shows high affinity for very low density lipoprotein particles (VLDLs).[4] Additionally, apoE3 and apoE4 bind to low-density lipoprotein receptors (LDLR) with high affinity, but apoE2 binds only weakly.[1−3] Importantly, apoE4 is associated with higher risk for Alzheimer's disease and for cardiovascular disease while apoE2 is associated with hyperlipoproteinemia.[3,5−17] In spite of the profound differences in the outcomes of these diseases, the differences in the molecular properties of the apoE isoforms are still unclear.

The complete structure of lipid-free wild-type ApoE is unknown, but the apoE monomer consists of two domains, an N-terminal domain (residues 1−191) and a C-terminal domain (residues 221−299).[18] The single amino acid changes occur in the N-terminal domain with apoE2 containing two cysteines (C112/C158), apoE4 with arginines replacing the two cysteines (R112/R158), and apoE3 containing a cysteine and an arginine at these two positions (C112/R158). The two domains are linked by a 40 amino acid protease-sensitive hinge region. The structure of the N-terminal domain, determined by both X-ray crystallography and solution NMR, consists of a compact four-helix bundle.[19,20] The structure of the C-terminal domain has not been determined but is considered to contain extensive helical content. The C-terminal domain is thought to mediate ApoE oligomerization,[21−23] and it is believed to contain the major lipid binding site.[22] There are extensive domain−domain interactions between the N- and the C-terminal domains in all of the isoforms of apoE.[24−27]

ApoE undergoes large structural changes upon binding to lipid. X-ray diffraction studies have shown that apoE reorganizes lipid vesicles to disk-like structures with the protein forming a double belt around the lipid disk.[28] Low-resolution structural characterization of the lipoprotein particles did not detect any differences between the apoE isoforms.[29] The kinetics of apoE−phospholipid interactions are found to be isoform specific[30] with differences in the behavior being proposed to be a consequence of differences in the stability of the N-terminal helix bundle of the apoE protein.[30] However, these differences were observed when only the N-terminal domain of apoE was used rather than the full-length protein.[30] It is well-known that lipid-free apoE undergoes self-association, but which molecular weight form of apoE bind to lipids is not known. Several authors have suggested that the self-association might influence lipidation of apoE.[31−34]

Received: December 17, 2010
Revised: January 26, 2011
Published: February 15, 2011

dx.doi.org/10.1021/bi1020106 | *Biochemistry* 2011, 50, 2550–2558

However, this issue has not been explored carefully due to lack of a clear understanding of the self-association behavior of apoE. Since the C-terminal domain of apoE is involved in both self-association and lipid binding, it is likely that these two processes are linked. Hence in order to understand the lipidation process of the apoE isoforms, the role of self-association in this process need to be taken into account.

The kinetics of phospholipid solubilization by apoE have been shown to occur in two phases.[30] The data have been interpreted with the first phase attributed to apoE finding lattice defects in the lipid vesicle and with the second phase being a conformational change during which the N-terminal helix bundle opens to form the belt-like structure.[30] Here, we propose a different mechanism to describe the kinetic behavior that involves the dissociation of higher molecular weight species to the monomeric form followed by binding to the lipid. We have recently shown that the self-association behavior of apoE can be described as a monomer−dimer−tetramer process and have determined the association and dissociation rate constants.[35] At micromolar concentrations, where lipid binding experiments are frequently performed, apoE exists primarily as tetramers. Surprisingly, we find that the rate of dissociation of the tetramer to monomer and the rate of reorganization of the lipid by apoE appear to be the same. Thus we suggest that the slow kinetics of lipid binding is a consequence of slow dissociation of the apoE protein and that differences in the lipidation kinetics of the apoE isoforms arise from their differences in the self-association behavior.

MATERIALS AND METHODS

Materials. ApoE was prepared and purified as described previously.[27] Site-directed mutations were introduced by the QuickChange site-directed mutagenesis kit (Stratagene). The sequences of mutant proteins were verified by DNA sequencing. All chemicals used were Ultrapure from Sigma-Aldrich (St. Louis, MO).

Preparation of Unilamellar Liposomes. Small unilamellar vesicles (SUV) of dimyristoyl-*sn*-glycero-3-phosphocholine (DMPC) were prepared by extrusion through 50 nm polycarbonate membranes (Avanti Polar Lipids Inc.) followed by centrifugation at 14000*g*. These liposomes, when tested by light scattering, are stable for several days at room temperature.

Passivation of Cuvette Surface. To avoid adsorption of apoE, the inner surface of the quartz cuvette used for fluorescence experiments was passivated according to Selvin and Ha.[36] Briefly, the cuvette interior was thoroughly cleaned and then functionalized with (3-aminopropyl)triethoxysilane (Sigma). The surface passivation reaction was carried out with methoxy-poly(ethylene glycol)-succinimidyl valerate (mPEG-SVA; Laysan Bio Inc.) in bicarbonate buffer at pH 8.3.

Fluorescence Labeling of ApoE4. Alanine at position 102 in apoE4 was mutated to cysteine for fluorescent labeling. This single cysteine of apoE4 was labeled by either Alexa488 maleimide or Alexa546 maleimide or pyrene maleimide (Invitrogen). The protein at 2 mg/mL was dissolved in 50 mM HEPES buffer, pH 7.4, 6 M urea, and 200 μM tris(2-carboxyethyl)phoshine (TCEP) and then degassed under vacuum for 20 min. Alexa488 maleimide or Alexa546 maleimide or pyrene maleimide, 200 μM, was added and the solution kept dark at room temperature under vacuum for 2 h and then at 4 °C overnight. Excess dye was removed by passing the sample over a Superdex200 column in 4 M GdnCl (guanidine hydrochloride), 20 mM HEPES buffer, pH 7.4, and 0.1% β-mercaptoethanol (βMe). The labeled apoE was then refolded by dialysis against 20 mM HEPES buffer, pH 7.4, and 150 mM NaCl at 4 °C overnight. The absorbance of this sample at 280 and 490 nm (for Alexa488) or 555 nm (for Alexa546) or 335 nm (for pyrene) was used to determine the labeled fraction. For all of the samples the labeling efficiency was greater than 90%.

Turbidity Measurements. Various concentrations of WT apoE4 or apoE3 or apoE2 were added to 3 mL of HEPES buffer (20 mM HEPES, 150 mM NaCl, 0.1% βMe, and pH 7.4) and let stand at room temperature for 2 h. DMPC liposomes (final concentration = 0.25 mg/mL) were added to the apoE solutions, and the solution was stirred continuously throughout the experiments. The turbidity clearance of the DMPC liposomes was performed by monitoring scattering from the sample at 90° to the incident light using an Alphascan fluorometer (Photon Technology International, Inc.) equipped with a programmable shutter. The wavelength of light used in both the excitation and the emission channel was set to 600 nm.

Intermolecular FRET Experiments. Separate apoE4-labeled proteins with either Alexa488 or Alexa546 were mixed at a ratio of 1:3 in 4 M GdnCl. This sample was then dialyzed at 4 °C in 20 mM HEPES buffer, pH 7.4, and 150 mM NaCl, flash frozen in liquid nitrogen in small aliquots (100 μL), and then stored at −80 °C prior to use. FRET kinetic experiments were performed using the fluorometer with the excitation and emission monochromators set to 490 and 520 nm, respectively. For these experiments different amounts of labeled apoE4 stock solution (from 6 to 48 μL of 10 μM apoE4) were added into 3 mL of buffer containing DMPC liposomes (final concentration = 0.25 mg/mL) and mixed within 2−3 s. The solutions were stirred continuously throughout the experiments. The fluorescence was then monitored for ≈2 h. To prevent photobleaching, the shutter in the excitation light path was closed between measurements. All experiments performed at 25 °C.

Intramolecular FRET Experiments. For the denaturation experiments apoE4 labeled with pyrene at position 102 was diluted into 20 mM HEPES, 150 mM NaCl, 0.1% βMe, and pH 7.4 buffer containing varying concentrations of urea. The final apoE concentration was 110 nM. The tryptophan fluorescence at 340 nm with excitation at 290 nm was recorded at each urea concentration. Nonlinear least-squares fit was performed using Origin 7.0 (Origin Laboratories, USA) with a two-state model using the six-term equation adapted from Santoro and Bolen.[37] For the kinetic experiments, 110 nM pyrene-labeled apoE4(A102C) was added to 3 mL of HEPES buffer containing DMPC liposomes (final concentration = 0.25 mg/mL) and mixed within 2−3 s. The tryptophan fluorescence was then monitored for ≈2 h. The solution was stirred continuously throughout the experiment. To minimize photobleaching, the shutter in the excitation light path was closed between measurements. All experiments performed at 25 °C.

Analysis of Kinetic Data. The kinetics of lipidation data were analyzed using the model in Scheme 1 by Kintek Explorer (KinTek Corp.).[38]

Denaturation Experiments Using Circular Dichroism. For urea denaturation studies with CD an apoE stock solution (20−30 μM) in Hepes buffer was diluted 10-fold into 20 mM phosphate and pH 7.4 buffer containing varying concentrations of urea. CD spectra were recorded using a Jasco J-715 spectropolarimeter. Twelve scans from 225 to 220 nm with a speed of 20 nm/min were averaged for all samples. The fraction (F) of unfolded population was calculated from

$$F = \frac{\theta - \theta_U}{\theta_N - \theta_U} \quad (1)$$

Scheme 1. ApoE−Lipid Interaction Model[a]

$$m_4 \underset{k_{+2}}{\overset{k_{-2}}{\rightleftharpoons}} m_2 + m_2;\ m_2 \underset{k_{+1}}{\overset{k_{-1}}{\rightleftharpoons}} m_1 + m_1$$

$$m_1 + L \underset{k_{-b}}{\overset{k_{+b}}{\rightleftharpoons}} MI;\ MI \underset{k_{-c}}{\overset{k_{+c}}{\rightleftharpoons}} ML$$

[a] m_1, m_2, and m_4 represent monomer, dimer, and tetramer of apoE, respectively. L represents phospholipid, MI is an intermediate, and ML is the final lipidated apoE.

where θ is the CD signal at 222 nm and U and N indicate unfolded and native state, respectively. Nonlinear least-squares fit is performed using Origin 7.0 (Origin Laboratories, USA) with a three-state model using the equation adapted from ref 39.

RESULTS

Role of Self-Association in Lipidation of ApoE. We have previously characterized the concentration-dependent self-association behavior of apoE.[35] At micromolar concentrations, tetramers are the dominant species while at lower concentrations (<200 nM) monomers and dimers predominate. However, the dissociation of the tetramers, and specifically the dissociation of dimers to monomers, is a slow process typically taking more than 1 h.[35] To test the hypothesis that the oligomeric state of apoE influences its binding to lipid, kinetic experiments were performed with apoE at different starting concentrations (and therefore different oligomeric states) but with the same final concentration. When lipid-free apoE is added to a turbid solution of vesicles of phospholipids, the turbidity decreases in a time-dependent manner due to conversion of the vesicles to small disk-like lipoprotein particles (radius ~5−6 nm) induced by apoE.[28−30,40] Figure 1 shows that the rate of turbidity clearance of DMPC liposome solutions upon addition of wild-type apoE4 is different depending on the initial concentration of the protein even though the final concentration was the same. Thus, the only difference at time zero is the oligomeric distribution of apoE. When apoE solutions were preequilibrated at 65 nM (or at 260 nM) prior to adding the DMPC vesicles, the rate of vesicle clearance was faster than when apoE incubated at 27 μM was added to vesicles at the start of the experiments. We interpret the differences in rates to originate from the different initial distribution of oligomeric species. Thus when apoE is preincubated at 65 nM (or at 260 nM), monomers and dimers predominate while at 27 μM there are only tetramers present.[35] This experiment shows that either the monomer or the dimer but not the tetramer interacts with the liposomes.

Reaction Scheme of ApoE−Lipid Interactions. A complete reaction scheme for the binding of apoE to lipid would include the possibility that all oligomeric forms of apoE are capable of binding. Figure 1 suggests that the tetrameric forms must dissociate before apoE binding to lipid can occur. This might be an expected result because oligomerization is believed to occur via the C-terminal domain in regions similar to lipid binding domains.[22] If we further assume (as discussed later) that dimer formation also involves the same domain, the simplest mechanism would involve only monomer binding to lipid. This mechanism is shown in Scheme 1. In this scheme we include the self-association properties of lipid-free apoE.[35] We then assume that only monomers bind to lipids and that the binding process is rapid and reversible. Since it is known that lipid binding leads to

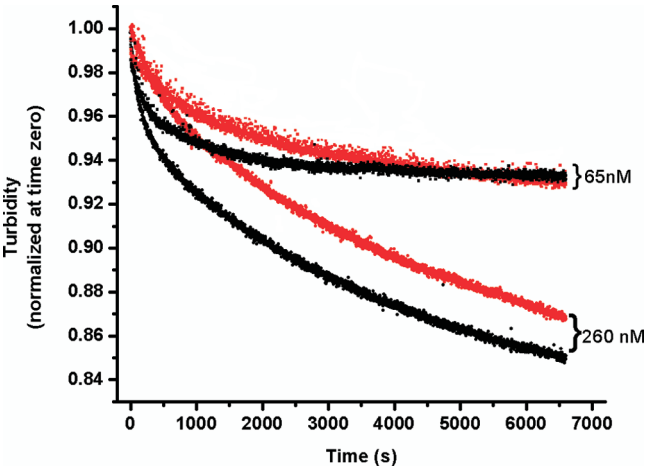

Figure 1. Effect of apoE self-association state on solubilization of DMPC liposomes. Turbidity measured by scattering from DMPC liposomes was followed after addition of WT apoE4, either equilibrated at the final concentrations (black) or diluted from 27 μM stock solution directly (red) into 0.25 mg/mL DMPC, 20 mM HEPES, 150 mM NaCl, 0.1% βMe, and pH 7.4 buffer. The final concentrations of apoE were 65 or 260 nM. Scattering from the sample at 90° to the incident light was monitored at 600 nm.

transformation of the lipid vesicles to small disk-like particles and a large conformational change in apoE,[28] we include an irreversible step to reflect this conformational change. While a detailed mechanism of apoE−lipid interaction is not known, it is generally believed that interaction of apoE to lipoprotein particles occurs through two steps. The initial binding (first step) through the C-terminal domain is considered rapid and reversible.[30,41−43] This is followed by opening of the N-terminal helix bundle whereby helix−helix interactions are converted to helix−lipid interactions. This second step is relatively slow and is not readily reversible.[43] For simplicity we assumed that the off rate constant (k_{-c}) for this confomational conversion step is sufficiently close to zero that we can set it to zero. As we will show later, this assumption works well to describe the experimental data. We also note that while the actual process of binding to lipids and conformation change of the apoE molecules may occur simultaneously, these processes are treated sequentially in the kinetic scheme. We have previously determined the rate constants (k_{-1}, k_{+1}, k_{-2}, k_{+2}) governing the self-association process under the conditions of these experiments.[35] In order to simulate the data, the on and off rate constants (k_{+b} and k_{-b}, repectively) for apoE−lipid binding were fixed at 10^6 M^{-1} s^{-1} and 1 s^{-1}, values considered to signify that the lipid binding is fast and reversible. The determination of the values of k_{+b} and k_{-b} is beyond the scope of this paper; hence, these values are somewhat arbitrary. The forward rate constant (k_{+c}) for the conformational change of apoE is unknown and will be determined by experiments given in the subsequent sections.

Comparison of Lipidation Kinetics with Monomer Formation. To test the lipidation model proposed in Scheme 1, the kinetics of liposome clearance were compared with the kinetics of dissociation of the tetramers to monomers. Figure 2 shows the kinetic data for liposome clearance by 65 nM apoE4 diluted from a 27 μM stock solution at the start of the experiment. Superimposed is the formation of monomer (squares) calculated using the rate constants for the self-association process of apoE4 determined under the same experimental conditions.[35]

As discussed above, we assumed fast and reversible binding of the monomer to the liposomes. It is clear from Figure 2 that the liposome clearance data correlate well with the formation of monomers from the tetramers.

Concentration Dependence of ApoE Self-Association. To determine the rate constant for the conformational change of apoE and to test the applicability of the proposed reaction scheme, the kinetics of apoE−lipid interaction experiments were performed as a function of apoE concentration. Turbidity clearance of DMPC liposomes by various concentrations of apoE4 is shown in Figure 3A. These data show that the rate of turbidity clearance increases as the concentration of apoE decreases. The experimental data can be fit with the reaction scheme presented in Scheme 1. To fit the experimental data, the on and off rate constants (k_{+b} and k_{-b}, repectively) for apoE−lipid binding were fixed at 10^6 M^{-1} s^{-1} and 1 s^{-1}, as discussed above. Although the values of the association−dissociation rate constants were set according to ref 35, the best fits were achieved by slight adjustments to the dissociation rate contants (viz., k_{-2} and k_{-1}). The analysis also allows determination of the forward rate constant of the conformational change (k_{+c}) of the apoE monomer (see Table 1). Similar experiments and analysis performed using apoE3 and apoE2 are shown in panels B and C of Figure 3, respectively. It is clear that the experimental data agree well with the proposed scheme. The analysis shows that the rate constants for the association−dissociation process and for conformational changes of apoE are different for the isoforms (Table 1), indicating the isoform-specific nature of apoE−lipid interaction. We note here that there are small deviations in the fits at the early time points (<200 s). The cause of this deviation is not clear but may be a consequence of a rapid change in the state of the liposomes immediately after mixing with apoE.

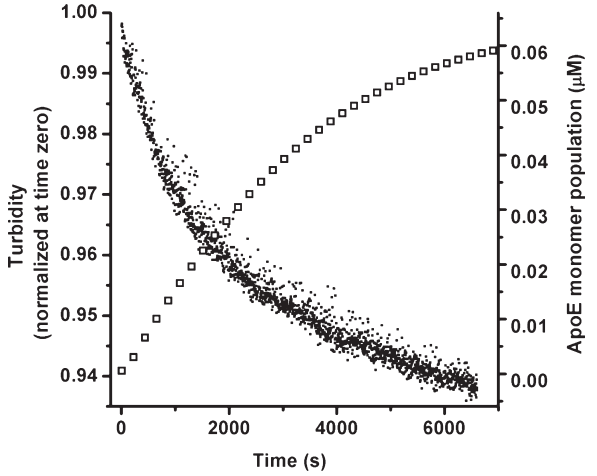

Figure 2. Comparison of liposome solubilization and dissociation of the tetramers of apoE. Turbidity measured by scattering (dots) from DMPC liposomes followed by addition of 65 nM WT apoE4 diluted from 27 μM stock solution into a 0.25 mg/mL DMPC liposome solution in 20 mM HEPES, 150 mM NaCl, 0.1% βMe, and pH 7.4 buffer. The concentration of monomers (□) as a function of time was calculated using previously determined association and dissociation rate constants of lipid-free apoE[35] and assuming fast and reversible binding of the apoE monomer to the liposomes. The kinetic traces were made using Kintek Explorer (Kintek Corp.).[38]

Kinetics of Dissociation and Lipidation Using Intermolecular FRET. We have previously used intermolecular FRET to monitor the rate of dissociation of apoE multimers after dilution and to establish a self-association scheme of lipid-free apoE.[35] Since the reaction scheme proposed here is an extension of the reaction scheme of the self-association of lipid-free apoE, we tested the validity of our current model using change in the FRET signal in the presence of DMPC liposomes. In contrast to the turbidity clearance studies, these experiments measure the dissociation of apoE. The changes in the FRET signal at various concentrations of labeled apoE4 in the presence of DMPC liposomes are shown in Figure 4. In these experiments apoE4 labeled with either Alexa488 (fluorescence donor) or Alexa546 (fluorescence acceptor) was mixed, equilibrated, and diluted in the buffer containing DMPC liposomes, and the fluorescence of Alexa488 was monitored as a function of time. The slow rate of dissociation agrees well with the data presented in Figures 1−3. The solid lines are simulated using the rate constants for apoE4 listed in Table 1. Figure 4 shows that the FRET data are in agreement with the rate constants obtained from the analysis of the turbidity clearance data.

Kinetics of Turbidity Clearance and the Conformational Change of ApoE. It is known that apoE undergoes large conformational change on binding to lipid.[28] Since apoE monomer contains seven tryptophan residues in its sequence, four in the N-terminal domain and three in the C-terminal domain, FRET between the tryptophans and an acceptor dye in a suitable position in the sequence can be used to monitor the conformational changes of the apoE molecule. We have used pyrene-labeled apoE4 (A102C) and detected a significant amount of FRET signal between the pyrene and the native tryptophan residues.

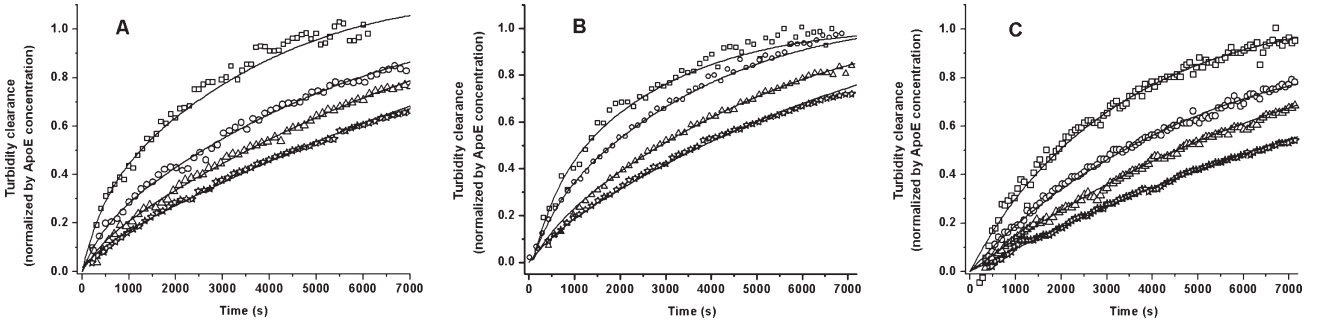

Figure 3. Concentration dependence of turbidity clearance by the apoE isoforms. Turbidity clearance by 88 nM (□), 176 nM (○), 352 nM (△), and 700 nM (star) WT apoE4 (A), WT apoE3 (B), or WT apoE2 (C) of 0.25 mg/mL DMPC liposome solution in 20 mM HEPES, 150 mM NaCl, 0.1% βMe, and pH 7.4 buffer. The solid lines were fit to the data using the model shown in Scheme 1 and the rate constants listed in Table 1. Scattering from the sample at 90° to the incident light was monitored at 600 nm.

dx.doi.org/10.1021/bi1020106 |*Biochemistry* 2011, 50, 2550–2558

Table 1. Summary of Rate Constants[a]

sample	k_{+1}[b] (M^{-1} s^{-1})	k_{-1}[b] (s^{-1})	k_{+2}[b] (M^{-1} s^{-1})	k_{-2}[b] (s^{-1})	k_{+c} (s^{-1})
WT apoE4	8.5×10^3	6.4×10^{-4}	2.0×10^5	4.0×10^{-3}	$(2.4 \pm 0.2) \times 10^{-3}$
WT apoE3	4.7×10^3	5.4×10^{-4}	0.8×10^5	5.0×10^{-3}	$(2.0 \pm 0.2) \times 10^{-3}$
WT apoE2	6.0×10^3	4.6×10^{-4}	0.8×10^5	5.0×10^{-3}	$(1.0 \pm 0.2) \times 10^{-3}$

[a] The rate constants k_{+b} and k_{-b} are fixed at 10 M^{-1} s^{-1} and 1.0 s^{-1}, respectively. [b] The values of k_{+1}, k_{-1}, k_{+2}, and k_{-2} are derived from ref 35. The value of k_{-1} for apoE2 was varied by more than 10% to fit the data presented in Figure 3.

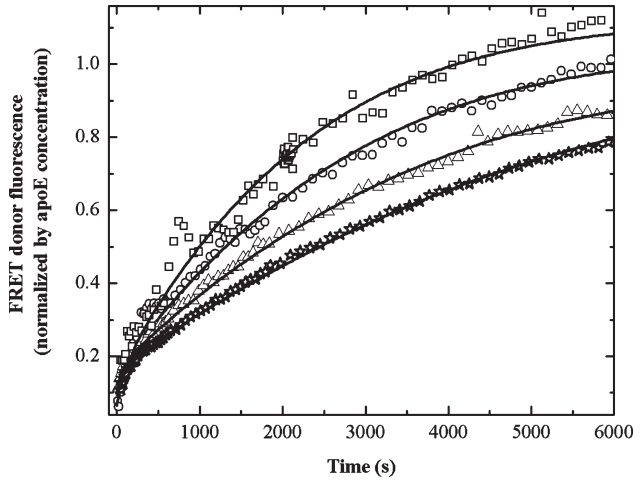

Figure 4. Kinetics of dissociation of Alexa488- and Alexa546-labeled apoE4 in the presence of DMPC liposomes using intermolecular FRET. Fluorescently labeled apoE4 (15 μM) was diluted to final concentrations of 25 nM (□), 50 nM (○), 100 nM (△), and 200 nM (star) into 0.25 mg/mL DMPC liposome solution in 20 mM HEPES, 150 mM NaCl, 0.1% βMe, and pH 7.4 buffer. The molar ratio of Alexa488- and Alexa546-labeled apoE4 (A102C) used was 1:3. The excitation and emission wavelengths were 490 and 520 nm. The solid lines were calculated using the rate constants shown in Table 1 for apoE4 by Kintek Explorer.[38]

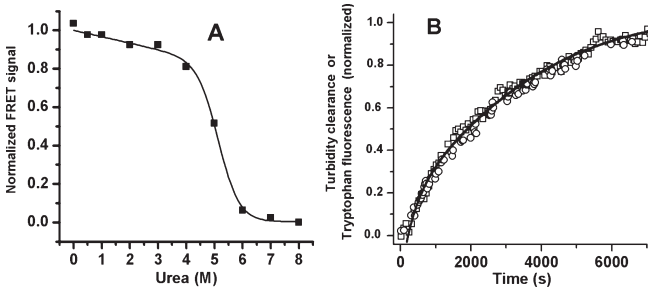

Figure 5. Denaturation of pyrene-labeled apoE measured by FRET and kinetics of lipidation monitored by FRET and turbidity clearance. (A) FRET between pyrene at position 102 and tryptophans in pyrene-labeled apoE4 (A102C) as a function of urea concentrations (squares). The solid line represents a fit to the denaturation data using a two-step model according to ref 37. (B) Kinetics of lipidation of pyrene-labeled apoE4 (A102C) as monitored by FRET (○) or by turbidity clearance (□). The solid line was calculated from the rate constants for apoE4 as shown in Table 1. The concentration of apoE4 used was 110 nM. FRET signal was monitored at 340 nm with excitation at 290 nm, and scattering was monitored at 600 nm.

In order to understand the nature of the structural changes observed by changes in the FRET signal, we performed denaturation of pyrene-labeled apoE4 (102C) by monitoring the

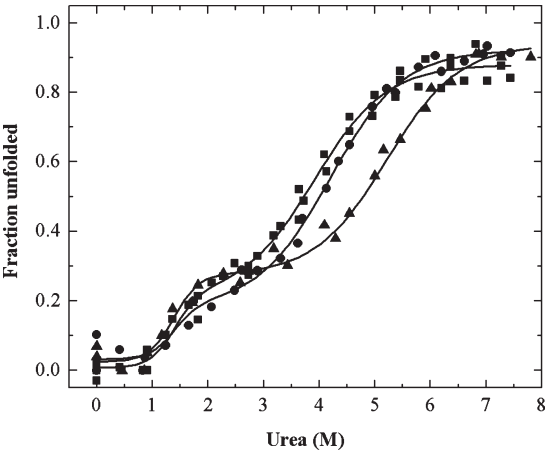

Figure 6. Urea denaturation of apoE isoforms measured by circular dichroism at 222 nm. The normalized unfolded fraction of apoE is plotted as a function of urea concentration for WT apoE4 (■), apoE3 (●), and apoE2 (▲). The solid lines are fits to the data using a three-state denaturation model according to ref 39.

FRET signal. Figure 5A shows that the tryptophan fluorescence of pyrene-labeled apoE4 increases with denaturation by urea, indicating loss of FRET due to denaturation. This is to be expected since the tertiary structure of the protein molecule loses compactness and adopts more extended form. The midpoint of denaturation is ≈5 M, close to the denaturation midpoint of the N-terminal domain of apoE4.[44] The observed FRET signal may be a sum of intermolecular, interdomain, or intradomain energy transfer between the native tryptophans and the pyrene. The FRET signal change at 3 M urea, however, is less than 20% of the total, and this urea concentration is sufficient to unfold the C-terminal domain[44] and to dissociate the multimers of apoE.[27] Thus the contributions from self-association and domain−domain proximity are small, and the observed FRET can be considered intramolecular involving only the tryptophans of the N-terminal domain. The change in FRET signal may therefore be used to monitor structural unfolding of the N-terminal domain of apoE in the presence of the DMPC liposomes.

Figure 5B compares the relation between the kinetics of turbidity clearance (squares) and the kinetics of the conformational changes by intramolecular FRET (circles) due to lipidation of apoE. The observed loss of FRET signal on addition of the protein to the lipid vesicles indicates an increase in distance between the pyrene and the tryptophans at the N-terminal domain of apoE, as the α-helices of the apoE molecules are stretched on the surface of the lipid molecules as opposed to the more compact helix bundle conformation in the lipid-free state.[28] It is clear from these data that the kinetics of conformational changes and of the turbidity clearance are essentially identical. In addition, the kinetic data agree well with the rate constants (solid line) as summarized in Table 1.

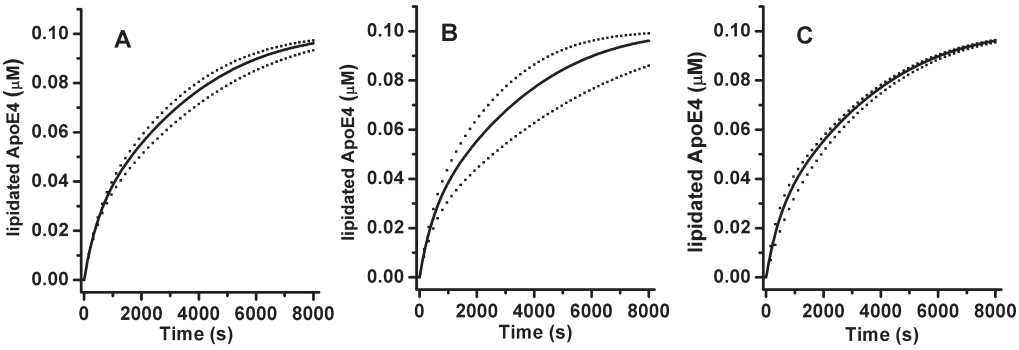

Figure 7. The rate-determining process in lipidation of apoE. The kinetics of lipidation of 100 nM apoE4. The solid line is calculated using the rate constants listed in Table 1 for apoE4. The other kinetic plots are calculated assuming a 33% variation in the values of k_{-2} (A) or k_{-1} (B) or k_{+c} (C). It can be seen that the dissociation rate constant of dimer to monomer (k_{-1}) has the maximum effect on the overall rate. The kinetic traces are generated using Kintek Explorer.[38]

Forward Rate Constant of Conformational Change (k_{+c}) and Denaturation Stability. To test whether the measured forward rate constants for the conformation change (k_{+c}) of the monomeric apoE molecule can be related to the stabilty of different apoE isoforms, we performed denaturation experiments of the apoE isoforms. The urea denaturation profiles of WT apoE4, apoE3, and apoE2, as measured by circular dichroism at 222 nm, are shown in Figure 6. The denaturation data for all of the isoforms show three-state unfolding behavior corresponding to the unfolding of the C-terminal domain at low urea concentrations followed by the unfolding of the N-terminal domain at higher urea concentrations as has been shown by others.[44] The denaturation data are fit according to Morjana et al.[39] using a three-state model. It can be seen that the apoE2 is the most stable among all of the isoforms followed by apoE3 and apoE4. However, the differences in the stabilities between apoE3 and apoE4 appear small. This is in agreement with the measured k_{+c} values (see Table 1) for each of the isoforms where the differences are small between apoE3 and apoE4 but large between apoE2 and the other two isoforms. Hence the rate constant of conformational changes (k_{+c}) of the apoE monomer is correlated with its denaturation stability.

DISCUSSION

Reaction Scheme of ApoE−Lipid Interaction. The clearance of DMPC liposomes has been shown to occur in two steps.[30] The data have previously been intrepreted as a fast binding step followed by a slow conformational change.[30] Our data show that this interpretation is incorrect because the role of oligomerization was ignored. Thus, we conclude that the fast phase is a monomer binding step and the slow phase is the dissociation of oligomeric species to the monomer that is then followed by the conformational change. While the kinetic data presented in Figures 1 and 2 support this idea, the reaction mechanism in Scheme 1 can be tested more rigorously by the quantitative analysis of the kinetics of lipidation at various concentrations of apoE. Figures 3−5 clearly show that the data are consistent with the proposed model using the previously determined rate constants of association−dissociation processes of apoE. These experiments further enable us to determine the rate constants of conformational changes of apoE molecules on lipid binding.

Only Monomer Binds to Lipids. Our model proposes that only the monomer of apoE binds tightly to the lipid vesicle. Efforts to fit the experimental data shown in Figures 3 and 4 by assuming that only dimers bind to lipids were not successful. However, it is known that there is more than one apoE molecule in a lipoprotein particle. For example, apoE−DPPC particles contain at least two apoE molecules that exist as separate monomers.[28] It is possible that after binding to the liposome surface two apoE molecules diffuse closer before formation of the fully formed lipoprotein particle. While our data are consistent with only monomers of apoE binding to lipids, the possibility exists that dimers may bind and then undergo dissociation to monomers on the liposome surface. The kinetic experiments presented here do not distinguish between these two possibilities, but it is evident from our data that dissociation of the apoE oligomers to monomers is necessary for formation of the final lipoprotein particles. We also note here that it is possible that multiple binding modes exist for apoE−phospholipid interaction. Hence it is possible that higher ologimers of apoE also bind to lipids but with lower affinity. This is particularly relevant since the isolated N-terminal domain also binds to lipids.[30]

Rate-Limiting Factor in the ApoE−Lipid Interaction Process. As noted earlier, the reaction model in Scheme 1 includes the rate constants for the association−dissociation process and the apoE−lipid interaction process. Modest variations in the values of the association rate constants (k_{+1} and k_{+2}) and the rate constants for apoE−lipid binding step (k_{+b} and k_{-b}) do not seem to alter the conclusions (data not shown). However, changes in dissociation rate constants of the tetramers and the dimers (k_{-2} and k_{-1}, respectively) and changes in the forward rate constant of the conformational change of the apoE monomer (k_{+c}) do affect the lipidation kinetics significantly. Changes in the lipidation kinetics using the same amount of deviation (±33%) from the mean value of k_{-2} or k_{-1} or k_{+c} are shown in Figure 7, while keeping all of the other rate constants the same. These plots have been generated by Kintek Explorer (Kintek Corp.)[38] at 100 nM apoE4 and 0.25 mg/mL DMPC using the rate constants listed in Table 1. It can be seen that changes in k_{-2} or k_{-1} or k_{+c} influence the kinetics with k_{-1} having the most pronounced effect. Since only the monomers bind to lipids, it is intuitive that the dissociation of the dimer to the monomer is the rate-limiting step.

Comparison of the ApoE Isoforms. The analysis presented here using the mechanism in Scheme 1 makes it possible to separate the contributions of self-association from that of the conformational change. Table 1 shows that the forward rate constant for the conformation conversion of the monomeric form of apoE is isoform specific and that these rate constants

appear to be correlated with the relative denaturation stabilities of these proteins. However, it is clear from Figure 7 that the dissociation of the dimers to the monomers is the rate-determining step at concentrations near or above 100 nM apoE. Table 1 shows that the rate constants for dissociation of dimers to monomers (k_{-1}) are different for the isoforms, being fastest for apoE4 and slowest for apoE2. Hence the isoform specificity of the kinetics of lipidation is dictated by the isoform specificity of the self-association process. The isoform-specific behavior of the kinetics of lipidation has previously been assumed to arise from the isoform-specific denaturation stability of the apoE isoforms. This interpretation worked well when only the N-terminal domain (residues 1−191) was used but not when the full-length apoE was used.[30] We can explain this using our observation that the association−dissociation behavior determines the kinetics of lipidation for the full-length apoE, but in the absence of self-associtation which is the case for the N-terminal domain alone the stability of the N-terminal domain would determine the kinetics of lipidation.

Conformational Changes and Lipidation. As is well-known apoE molecules undergo a large confomation reorganization due to lipidation.[28] However, the rate of conformational changes and the rate of solubilization of the liposomes have not been previously compared. The data as presented in Figure 5B show that these two processes have similar time scales, indicating that the conformational conversion and the formation of the lipidated apoE particles are simultaneous.

Is the interplay of self-association of apoE and the apoE−lipid interaction important *in vivo*? While lipid-free apoE is not found in the plasma, a large amount of apoE synthesized by the macrophages is thought to be lipid-poor and self-associated.[45] ApoE secreted by HEK cells transfected with human apoE is found to be essentially lipid-free and exists as tetramers.[46] ATP binding cassette protein ABCA1 which plays important role in the lipidation of apoE binds to lipid-free apoE more efficiently than lipidated apoE.[47] In addition, lipid-free apoE is biologically active, capable of causing cholesterol efflux and of binding to several cell surface receptors such as ABCA1, lipoprotein receptor related protein (LRP), very low density lipoprotein receptor (VLDL receptor), and heparin sulfate proteoglycans (HSPG).[45,47−54] These observations indicate that lipid-free apoE is biologically relevant and self-association behavior of lipid-free apoE may have consequences in the lipidation of apoE *in vivo*. In addition, differences in the self-association behavior of the apoE isoforms can explain some of the isoform-specific physiological properties of the apoE proteins.

In conclusion, here we present a new scheme to describe the interactions of apoE with phospholipids. In this scheme oligomers of apoE first need to dissociate to monomers before binding to lipids, a step that is then followed by a large conformational reorganization of the monomer. Prior knowledge of the rate constants of self-association of lipid-free apoE[35] enables us to interpret the kinetic data correctly and quantitatively. The data and the analysis presented here will help to advance our understanding of the molecular mechanism of lipoprotein particle formation of apoE and apolipoproteins in general.

AUTHOR INFORMATION

Corresponding Author

*E-mail: frieden@biochem.wustl.edu. Phone: (314) 362-3344. Fax: (314) 362-7183.

Funding Sources

This work is supported in part by NIH Grant DK13332 and by the Hope Center for Neurological Disorders at Washington University.

ACKNOWLEDGMENT

We thank Dr. Philip Vergesse for providing expertise with lipids and preparation of liposomes.

ABBREVIATIONS

apoE, apolipoprotein E; WT, wild type; GdnCl, guanidine hydrochloride; FRET, fluorescence resonance energy transfer; βMe, β-mercaptoethanol; DMPC, dimyristoyl-*sn*-glycero-3-phosphocholine; SUV, small unilamellar vesicle.

REFERENCES

(1) Weisgraber, K. H., Innerarity, T. L., and Mahley, R. W. (1982) Abnormal lipoprotein receptor-binding activity of the human E apoprotein due to cysteine-arginine interchange at a single site. *J. Biol. Chem. 257*, 2518–2521.

(2) Rall, S. C., Jr., Weisgraber, K. H., Innerarity, T. L., and Mahley, R. W. (1982) Structural basis for receptor binding heterogeneity of apolipoprotein E from type III hyperlipoproteinemic subjects. *Proc. Natl. Acad. Sci. U.S.A. 79*, 4696–4700.

(3) Davignon, J., Gregg, R. E., and Sing, C. F. (1988) Apolipoprotein E polymorphism and atherosclerosis. *Arteriosclerosis 8*, 1–21.

(4) Weisgraber, K. H. (1990) Apolipoprotein E distribution among human plasma lipoproteins: role of the cysteine-arginine interchange at residue 112. *J. Lipid Res. 31*, 1503–1511.

(5) Mahley, R. W., Huang, Y., and Rall, S. C., Jr. (1999) Pathogenesis of type III hyperlipoproteinemia (dysbetalipoproteinemia). Questions, quandaries, and paradoxes. *J. Lipid Res. 40*, 1933–1949.

(6) Getz, G. S., and Reardon, C. A. (2009) Apoprotein E as a lipid transport and signaling protein in the blood, liver, and artery wall. *J. Lipid Res. 50* (Suppl.), S156–S161.

(7) Mahley, R. W., Weisgraber, K. H., and Huang, Y. (2009) Apolipoprotein E: structure determines function, from atherosclerosis to Alzheimer's disease to AIDS. *J. Lipid Res. 50* (Suppl.), S183–S188.

(8) Heide, S., Manfred, K., Glaser, C., and Schulz, S. (2009) Apolipoprotein E (apoE) polymorphism: a risk factor for fatal coronary sclerosis? *Forensic Sci. Int. 192*, 62–66.

(9) Vaisi-Raygani, A., Rahimi, Z., Nomani, H., Tavilani, H., and Pourmotabbed, T. (2007) The presence of apolipoprotein epsilon4 and epsilon2 alleles augments the risk of coronary artery disease in type 2 diabetic patients. *Clin. Biochem. 40*, 1150–1156.

(10) Winkler, K., Hoffmann, M. M., Krane, V., Marz, W., Drechsler, C., and Wanner, C. (2010) Apolipoprotein E genotype predicts cardiovascular endpoints in dialysis patients with type 2 diabetes mellitus. *Atherosclerosis 208*, 197–202.

(11) Bennet, A. M., Di Angelantonio, E., Ye, Z., Wensley, F., Dahlin, A., Ahlbom, A., Keavney, B., Collins, R., Wiman, B., de Faire, U., and Danesh, J. (2007) Association of apolipoprotein E genotypes with lipid levels and coronary risk. *J. Am. Med. Assoc. 298*, 1300–1311.

(12) Anuurad, E., Lu, G., Rubin, J., Pearson, T. A., and Berglund, L. (2007) ApoE genotype affects allele-specific apo[a] levels for large apo[a] sizes in African Americans: the Harlem-Basset study. *J. Lipid Res. 48*, 693–698.

(13) Wagle, J., Farner, L., Flekkoy, K., Wyller, T. B., Sandvik, L., Eiklid, K. L., Fure, B., Stensrod, B., and Engedal, K. (2009) Association between ApoE epsilon4 and cognitive impairment after stroke. *Dementia Geriatr. Cognit. Disord. 27*, 525–533.

(14) Corder, E. H., Saunders, A. M., Strittmatter, W. J., Schmechel, D. E., Gaskell, P. C., Small, G. W., Roses, A. D., Haines, J. L., and Pericak-Vance, M. A. (1993) Gene dose of apolipoprotein E type 4 allele and the risk of Alzheimer's disease in late onset families. *Science 261*, 921–923.

(15) Drzezga, A., Grimmer, T., Henriksen, G., Muhlau, M., Perneczky, R., Miederer, I., Praus, C., Sorg, C., Wohlschlager, A., Riemenschneider, M., Wester, H. J., Foerstl, H., Schwaiger, M., and Kurz, A. (2009) Effect of APOE genotype on amyloid plaque load and gray matter volume in Alzheimer disease. *Neurology 72*, 1487–1494.

(16) Farrer, L. A., Cupples, L. A., Haines, J. L., Hyman, B., Kukull, W. A., Mayeux, R., Myers, R. H., Pericak-Vance, M. A., Risch, N., and van Duijn, C. M. (1997) Effects of age, sex, and ethnicity on the association between apolipoprotein E genotype and Alzheimer disease. A meta-analysis. APOE and Alzheimer Disease Meta Analysis Consortium. *J. Am. Med. Assoc. 278*, 1349–1356.

(17) Alberts, M. J., Graffagnino, C., McClenny, C., DeLong, D., Strittmatter, W., Saunders, A. M., and Roses, A. D. (1995) ApoE genotype and survival from intracerebral haemorrhage. *Lancet 346*, 575.

(18) Hatters, D. M., Peters-Libeu, C. A., and Weisgraber, K. H. (2006) Apolipoprotein E structure: insights into function. *Trends Biochem. Sci. 31*, 445–454.

(19) Wilson, C., Wardell, M. R., Weisgraber, K. H., Mahley, R. W., and Agard, D. A. (1991) Three-dimensional structure of the LDL receptor-binding domain of human apolipoprotein E. *Science 252*, 1817–1822.

(20) Sivashanmugam, A., and Wang, J. (2009) A unified scheme for initiation and conformational adaptation of human apolipoprotein E N-terminal domain upon lipoprotein binding and for receptor binding activity. *J. Biol. Chem. 284*, 14657–14666.

(21) Aggerbeck, L. P., Wetterau, J. R., Weisgraber, K. H., Wu, C. S., and Lindgren, F. T. (1988) Human apolipoprotein E3 in aqueous solution. II. Properties of the amino- and carboxyl-terminal domains. *J. Biol. Chem. 263*, 6249–6258.

(22) Westerlund, J. A., and Weisgraber, K. H. (1993) Discrete carboxyl-terminal segments of apolipoprotein E mediate lipoprotein association and protein oligomerization. *J. Biol. Chem. 268*, 15745–15750.

(23) Patel, A. B., Khumsupan, P., and Narayanaswami, V. (2010) Pyrene fluorescence analysis offers new insights into the conformation of the lipoprotein-binding domain of human apolipoprotein E. *Biochemistry 49*, 1766–1775.

(24) Narayanaswami, V., Szeto, S. S., and Ryan, R. O. (2001) Lipid association-induced N- and C-terminal domain reorganization in human apolipoprotein E3. *J. Biol. Chem. 276*, 37853–37860.

(25) Hatters, D. M., Budamagunta, M. S., Voss, J. C., and Weisgraber, K. H. (2005) Modulation of apolipoprotein E structure by domain interaction: differences in lipid-bound and lipid-free forms. *J. Biol. Chem. 280*, 34288–34295.

(26) Zhang, Y., Chen, J., and Wang, J. (2008) A complete backbone spectral assignment of lipid-free human apolipoprotein E (apoE). *Biomol. NMR Assign. 2*, 207–210.

(27) Garai, K., Mustafi, S. M., Baban, B., and Frieden, C. (2010) Structural differences between apolipoprotein E3 and E4 as measured by (19)F NMR. *Protein Sci. 19*, 66–74.

(28) Peters-Libeu, C. A., Newhouse, Y., Hall, S. C., Witkowska, H. E., and Weisgraber, K. H. (2007) Apolipoprotein E*dipalmitoylphosphatidylcholine particles are ellipsoidal in solution. *J. Lipid Res. 48*, 1035–1044.

(29) Schneeweis, L. A., Koppaka, V., Lund-Katz, S., Phillips, M. C., and Axelsen, P. H. (2005) Structural analysis of lipoprotein E particles. *Biochemistry 44*, 12525–12534.

(30) Segall, M. L., Dhanasekaran, P., Baldwin, F., Anantharamaiah, G. M., Weisgraber, K. H., Phillips, M. C., and Lund-Katz, S. (2002) Influence of apoE domain structure and polymorphism on the kinetics of phospholipid vesicle solubilization. *J. Lipid Res. 43*, 1688–1700.

(31) Massey, J. B., Gotto, A. M., Jr., and Pownall, H. J. (1981) Human plasma high density apolipoprotein A-I: effect of protein-protein interactions on the spontaneous formation of a lipid-protein recombinant. *Biochem. Biophys. Res. Commun. 99*, 466–474.

(32) Choy, N., Raussens, V., and Narayanaswami, V. (2003) Inter-molecular coiled-coil formation in human apolipoprotein E C-terminal domain. *J. Mol. Biol. 334*, 527–539.

(33) Lund-Katz, S., and Phillips, M. C. (0000) High density lipoprotein structure-function and role in reverse cholesterol transport. *Subcell. Biochem. 51*, 183–227.

(34) Zhang, Y., Vasudevan, S., Sojitrawala, R., Zhao, W., Cui, C., Xu, C., Fan, D., Newhouse, Y., Balestra, R., Jerome, W. G., Weisgraber, K., Li, Q., and Wang, J. (2007) A monomeric, biologically active, full-length human apolipoprotein E. *Biochemistry 46*, 10722–10732.

(35) Garai, K., and Frieden, C. (2010) The association-dissociation behavior of the apoE proteins: kinetic and equilibrium studies. *Biochemistry 49*, 9533–9541.

(36) Selvin, P. R., and Ha, T. (2008) *Single-molecule techniques: a laboratory manual*, Cold Spring Harbor Laboratory Press, Cold Spring Harbor, NY.

(37) Santoro, M. M., and Bolen, D. W. (1988) Unfolding free energy changes determined by the linear extrapolation method. 1. Unfolding of phenylmethanesulfonyl alpha-chymotrypsin using different denaturants. *Biochemistry 27*, 8063–8068.

(38) Johnson, K. A., Simpson, Z. B., and Blom, T. (2009) Global kinetic explorer: a new computer program for dynamic simulation and fitting of kinetic data. *Anal. Biochem. 387*, 20–29.

(39) Morjana, N. A., McKeone, B. J., and Gilbert, H. F. (1993) Guanidine hydrochloride stabilization of a partially unfolded intermediate during the reversible denaturation of protein disulfide isomerase. *Proc. Natl. Acad. Sci. U.S.A. 90*, 2107–2111.

(40) Pownall, H., Pao, Q., Hickson, D., Sparrow, J. T., Kusserow, S. K., and Massey, J. B. (1981) Kinetics and mechanism of association of human plasma apolipoproteins with dimyristoylphosphatidylcholine: effect of protein structure and lipid clusters on reaction rates. *Biochemistry 20*, 6630–6635.

(41) Jonas, A., and Drengler, S. M. (1980) Kinetics and mechanism of apolipoprotein A-I interaction with L-alpha-dimyristoylphosphatidylcholine vesicles. *J. Biol. Chem. 255*, 2190–2194.

(42) Jonas, A., Drengler, S. M., and Patterson, B. W. (1980) Two types of complexes formed by the interaction of apolipoprotein A-I with vesicles of L-alpha-dimyristoylphosphatidylcholine. *J. Biol. Chem. 255*, 2183–2189.

(43) Nguyen, D., Dhanasekaran, P., Phillips, M. C., and Lund-Katz, S. (2009) Molecular mechanism of apolipoprotein E binding to lipoprotein particles. *Biochemistry 48*, 3025–3032.

(44) Morrow, J. A., Segall, M. L., Lund-Katz, S., Phillips, M. C., Knapp, M., Rupp, B., and Weisgraber, K. H. (2000) Differences in stability among the human apolipoprotein E isoforms determined by the amino-terminal domain. *Biochemistry 39*, 11657–11666.

(45) Langer, C., Huang, Y., Cullen, P., Wiesenhutter, B., Mahley, R. W., Assmann, G., and von Eckardstein, A. (2000) Endogenous apolipoprotein E modulates cholesterol efflux and cholesteryl ester hydrolysis mediated by high-density lipoprotein-3 and lipid-free apolipoproteins in mouse peritoneal macrophages. *J. Mol. Med. 78*, 217–227.

(46) LaDu, M. J., Stine, W. B., Narita, M., Getz, G. S., Reardon, C. A., and Bu, G. (2006) Self-assembly of HEK cell-secreted apoE particles resembles apoE enrichment of lipoproteins as a ligand for the LDL receptor-related protein. *Biochemistry 45*, 381–390.

(47) Krimbou, L., Denis, M., Haidar, B., Carrier, M., Marcil, M., and Genest, J. (2004) Molecular interactions between apoE and ABCA1. *J. Lipid Res. 45*, 839–848.

(48) Weisgraber, K. H., Rall, S. C., Mahley, R. W., Milne, R. W., Marcel, Y. L., and Sparrow, J. T. (1986) Human apolipoprotein E. Determination of the heparin binding sites of apolipoprotein E3. *J. Biol. Chem. 261*, 2068–2076.

(49) Lin, C.-Y., Duan, H., and Mazzone, T. (1999) Apolipoprotein E-dependent cholesterol efflux from macrophages: kinetic study and divergent mechanisms for endogenous versus exogenous apolipoprotein E. *J. Lipid Res. 40*, 1618–1626.

(50) Bultel-Brienne, S. P., Lestavel, S., Pilon, A., Laffont, I., Tailleux, A., Fruchart, J.-C., Siest, G. R., and Clavey, V. R. (2002) Lipid free apolipoprotein E binds to the class B type I scavenger receptor I (SR-BI) and enhances cholesteryl ester uptake from lipoproteins. *J. Biol. Chem. 277*, 36092–36099.

(51) Narita, M., Holtzman, D. M., Fagan, A. M., LaDu, M. J., Yu, L., Han, X., Gross, R. W., Bu, G., and Schwartz, A. L. (2002) Cellular catabolism of lipid poor apolipoprotein E via cell surface LDL receptor-related protein. *J. Biochem. 132*, 743–749.

(52) Ruiz, J., Kouiavskaia, D., Migliorini, M., Robinson, S., Saenko, E. L., Gorlatova, N., Li, D., Lawrence, D., Hyman, B. T., Weisgraber, K. H., and Strickland, D. K. (2005) The apoE isoform binding properties of the VLDL receptor reveal marked differences from LRP and the LDL receptor. *J. Lipid Res. 46*, 1721–1731.

(53) Yamauchi, Y., Deguchi, N., Takagi, C., Tanaka, M., Dhanasekaran, P., Nakano, M., Handa, T., Phillips, M. C., Lund-Katz, S., and Saito, H. (2008) Role of the N- and C-terminal domains in binding of apolipoprotein E isoforms to heparan sulfate and dermatan sulfate: a surface plasmon resonance study. *Biochemistry 47*, 6702–6710.

(54) Neyen, C., Pluddemann, A., Roversi, P., Thomas, B., Cai, L., van der Westhuyzen, D. R., Sim, R. B., and Gordon, S. (2009) Macrophage scavenger receptor a mediates adhesion to apolipoproteins A-I and E. *Biochemistry 48*, 11858–11871.